CONF-850410-45

SCOPING SYSTEMS ANALYSIS OF A 350 MWt MODULAR LIQUID METAL COOLED REACTOR*

by

E. E. Morris
Reactor Analysis and Safety Division
Argonne National Laboratory
Argonne, IL 60439

S. K. Rhow, and D. M. Switick
General Electric
310 DeGuigne Drive
Sunnyvale, CA 94088

CONF-850410--45

DE85 012117

ABSTRACT

The systems analysis code SASSYS was used to explore the sensitivity of the system response to various inherent reactivity feedback mechanisms and design features for a small, liquid-metal-cooled reactor during the first 1000 s following the initiation of an unprotected loss-of-flow and/or loss-of-primary-heat-removal transient. The results show that to maximize the inherent safety of small, liquid-metal-cooled reactors, inherent feedback mechanisms should be accounted for in establishing design features such as the flow coastdown time constant and the control rod suspension system. The results also indicate insensitivity of the system response to the operation or non-operation of heat removal systems during the early part of an unprotected loss-of-flow transient.

INTRODUCTION

The systems analysis code SASSYS (1,2,3) is used to perform a scoping sensitivity analysis of unprotected loss-of-flow and/or loss-of-primary-heat-removal accidents for a preliminary conceptual design of a mixed-oxide fueled, 350 MWt, modular, liquid-metal-cooled, fast reactor. The objective is to provide guidance on the design approaches which enhance inherent safety. The reactor response is tracked for the first 1000 s following a postulated upset in the primary heat removal system. The calculations do not take credit for the functioning of any decay heat removal system. An important aspect of the present analysis is the augmenting of the reactivity feedbacks due to Doppler broadening, fuel axial expansion, and coolant density changes with models to estimate the feedbacks due to radial expansion caused by the heat-up of structural material within the core and changes in the relative position of the control rods and the core. In the loss-of-flow cases, the temperature drop across the intermediate heat exchanger is assumed to remain constant throughout the transient. In the combined loss-of-flow, loss-of-heat-sink cases, the temperature drop across the intermediate heat exchanger is held constant for 30 s and then decreases linearly to zero at 50 s. It should be noted that none of the cases represent a complete loss of coolant flow because of significant flow augmentation by natural circulation.

The results of the scoping analysis illustrates the importance of understanding various inherent reactivity feedback mechanisms in establishing design features such as the flow coastdown time constant and the control rod suspension system. Also, comparison of loss-of-flow calculations with combined loss-of-flow, loss-of-heat-sink cases indicates relative insensitivity of the system response to the rate of heat removal from the primary system during the first several minutes of a loss-of-flow transient.

MODELING

A few descriptive parameters for the reactor core appear in Table 1. The core model contains 8 channels, 6 for the driver fuel and 2 for the radial blankets. In addition, three separate bypass channels represent respectively the primary control, secondary control, and removable radial shield subassemblies. The primary coolant loop, schematized in Fig. 1, consists of an outlet plenum with a closed cover gas, an intermediate heat exchanger, a downcomer, a lower plenum, a pump, an inlet plenum, and a bypass pipe in parallel with the core and the bypass

*Work performed under the auspices of the U.S. Department of Energy.

Table 1
Reactor parameters.

Thermal Power	350 MW
Coolant Inlet Temperature	594 K
Coolant Outlet Temperature	724 K
Peak Linear Power	23.8 kW/m
Flowing Sodium Void Worth	1.9 $
Doppler Coefficient	0.0111
Number of Subassemblies	
Driver Fuel	48
Radial Blanket	66
Number of Pins per Subassembly	
Driver Fuel	271
Radial Blanket	127

channels. The downcomer pipe wall includes much of the mass of the fixed radial shield and the vessel wall. The bypass pipe models the flow through intersubassembly gaps and between the removable radial shield subassemblies and the core barrel. The operation of the pump is simulated by specifying the pump head as a function of time. In addition, rather than using a detailed model for the secondary sodium loop, the primary coolant temperature drop and the thermal center of the intermediate heat exchanger are specified as a function of time.

The correlation used to evaluate the radial expansion feedback has the form

$$\Delta\rho_{rex} = C_r[\Delta T_{in} + X_b(\Delta T_{out} - \Delta T_{in})]$$

where $\Delta\rho_{rex}$ is the reactivity change due to changes in the coolant inlet temperature T_{in} and in the coolant temperature T_{out} at the elevation of the above-core load pads. This correlation, suggested by Huebotter (4), can be interpreted as follows: If the reactor power-to-flow remains constant while the coolant inlet temperature increases, the core would be expected to undergo an axially uniform radial expansion. The magnitude of this expansion will depend on the coefficient of linear expansion for the core structural materials and should be approximately proportional to the change in the coolant temperature. Straightforward neutronics analysis can provide an estimate of the reactivity change per unit change in the core radius. Multiplying the reactivity change by the change in radius per unit change in temperature then provides a value for the constant C_r. If, in addition to the change in the core inlet temperature, the power-to-flow also increases, an additional contribution to the reactivity change would be expected. This contribution is represented by the product of C_r, X_b, and the change in the coolant temperature rise through the core. One would normally expect the constant X_b to be a number less than unity. Huebotter suggests that the value should be the ratio of the distance between the core support plate and the core axial midplane to the distance between the core support plate and the above-core load pads. As implemented here, ΔT_{out} is taken to be the average change in the structure temperature at the outlet of the driver fuel subassemblies.

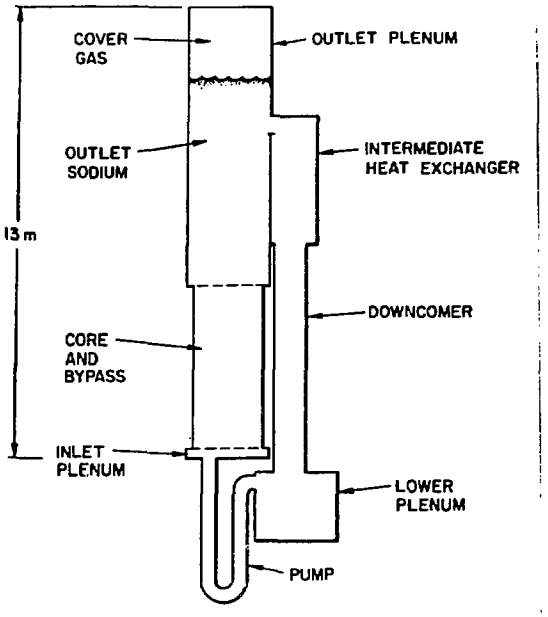

Fig. 1. Schematic of the primary coolant flow path.

The constant C_r was determined to have the value -0.338 cents/K. The constant X_b was determined by correlating radial expansion feedback as calculated by the CORTAC code (5) to the mixed mean coolant outlet temperature for the driver fuel subassemblies and was found to have the value 2. The CORTAC calculations used to determine X_b did not model changes in the core inlet temperature. Use of the structure temperature rather than the coolant temperature leads to a negligible error in the present analysis. A value greater than unity for X_b suggests that in addition to radial expansion, bowing of the fuel subassemblies is playing an important part in the radial expansion feedback in the CORTAC calculations. The uncertainty in the reactivity effects due to bowing should be kept in mind in interpreting the results of the analyses to be described later.

Reactivity feedback from the control rods in the absence of operator action can occur in at least two ways. First, as hot sodium enters the outlet plenum, it washes the control rod drive lines causing them to expand. This expansion can lower the rods into the reactor core and lead to a reduction in the net reactivity. Second, heating of sodium flowing next to the vessel wall can cause the vessel to expand and, depending on the system design, may increase the distance between the control rod supports and the core support plate. This can result in a withdrawal of the control rods and an increase in the net reactivity.

The SASSYS control rod drive line expansion model associates a specified sodium volume and a sodium-washed length with the control rod drive. The sodium temperature in the volume is

determined by assuming that the sodium flowing into the volume is exactly matched by sodium flowing out, that perfect mixing occurs with the incoming sodium, and that heat transfer occurs between the sodium and the control rod drive line. The initial temperature of the drive line and its associated sodium volume is set to the steady state temperature of the outlet plenum, and the temperature of the incoming sodium is taken as the mixed mean temperature of sodium leaving the subassemblies. Sodium leaves the volume with a temperature equal to the liquid temperature of the volume. The control rod drive line heat capacity, the coefficient for heat transfer between sodium and the control rod drive, and a coefficient of linear thermal expansion must also be specified.

The contribution of vessel expansion to the control rod feedback is estimated by assigning the average pipe wall temerature in the downcomer to the vessel wall. The change in this temperature is then multiplied by the wetted height of the vessel and the linear thermal expansion coefficient.

The change in reactivity due to relative motion of the core and control rods is computed as

$$\Delta\rho_{cont} = -K\,\Delta z$$

where

$$\Delta z = \Delta z_d - \Delta z_{ves},$$

Δz_d is the change in the control rod drive-line length, and Δz_{ves} is the change in the vessel wall length, both due to thermal expansion. The value K was set to 40 \$/m based on the total control rod worth assumed in the present analysis.

TRANSIENT ANALYSIS

Two cases with 3.6-s flow halving times are considered as reference cases. The only reactivity feedback mechanisms considered are Doppler, fuel-axial expansion, coolant density change, and core radial expansion. The first case has heat removal through the intermediate heat exchanger proportional to the primary coolant flow rate. The second is a combined loss-of-flow, loss-of-heat-sink transient. The thermal center and the geometric center of the intermediate heat exchanger are held coincident.

The total reactor power for the first case is shown as a function of time in Fig. 2. The power decreases monotonically with time, dropping below 10% of nominal within 260 s and to about 6% of nominal at the end of 1000 s. The reactivity feedbacks and the net reactivity for this case are shown in Fig. 3. The feedback components are easier to interpret with reference to temperature plots for a typical driver-fuel channel. Channel 1, which represents subassemblies near the center of the reactor is suitable for this purpose. Figure 4 shows the fuel-centerline, average, and outer-surface temperatures near the axial midplane as a function of time. While it is not readily apparent from the plot, the average temperature increases for a few seconds at the beginning of the transient, but then decreases for about 150 s. Thereafter, the fuel temperature gradually rises. As a result, both axial expansion and Doppler feedbacks are positive after

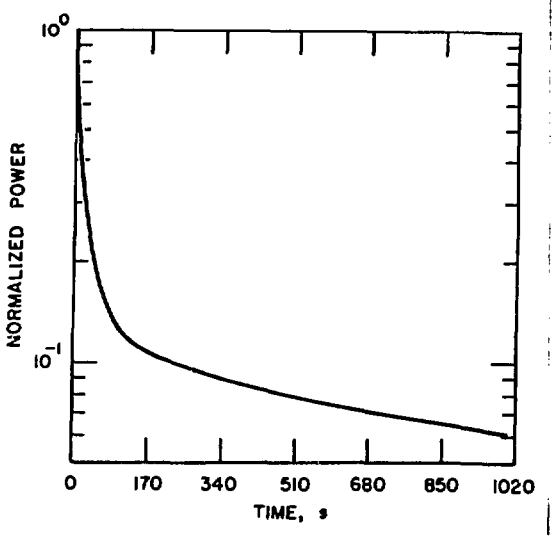

Fig. 2. Reactor power for loss-of-flow with no control rod reactivity feedback.

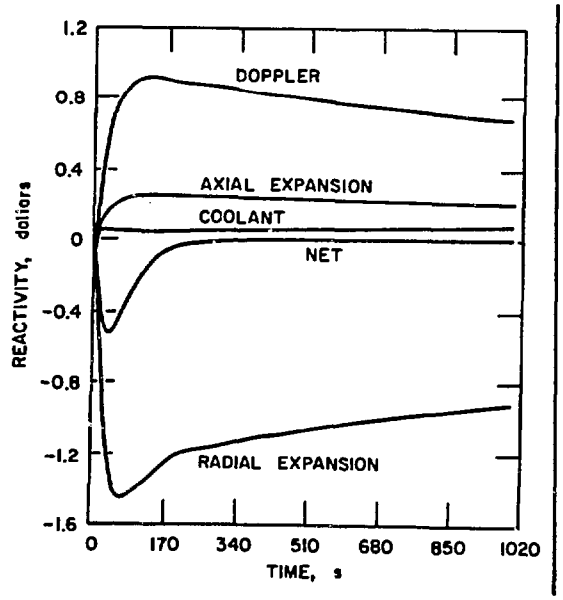

Fig. 3. Net and feedback reactivities for loss-of-flow with no control rod reactivity feedback.

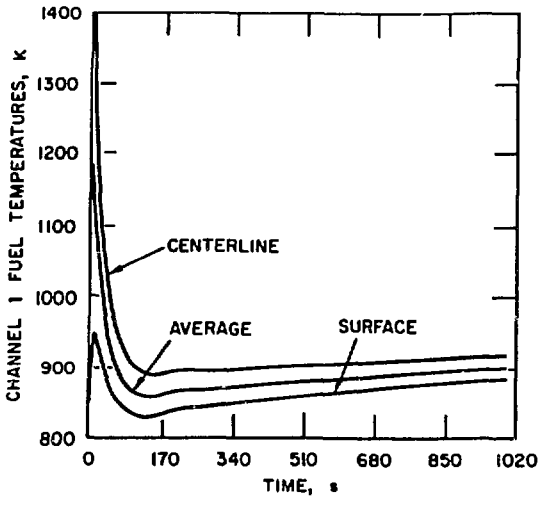

Fig. 4. Fuel temperatures for loss-of-flow with no control rod reactivity feedback.

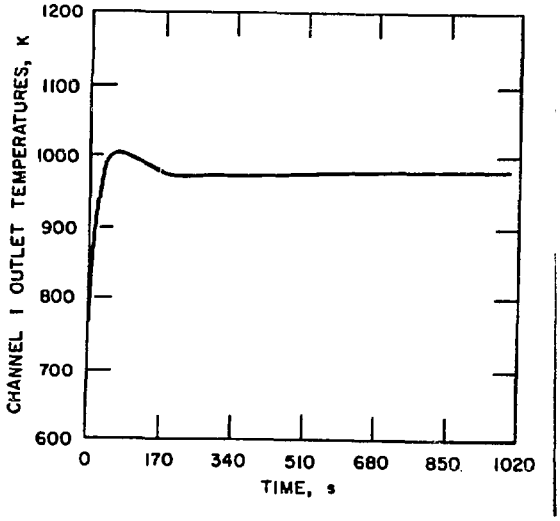

Fig. 5. Coolant outlet temperature for loss-of-flow with no control rod reactivity feedback.

about 10 s. The coolant density feedback is also positive, but plays a relatively minor role. These positive feedbacks are offset by negative feedback due to core radial expansion and subassembly bowing. Figure 5 shows the coolant and structure temperatures calculated near the outlet of channel 1. These temperatures rise from an initial value somewhat less than 750 K to nearly 1000 K during the first 60 s. The temperature increase leads to strong negative feedback such that the net reactivity remains negative or nearly zero throughout the transient. During the first 60 s, the inlet temperature increases only about 20 K, and thus, contributes relatively little to the radial expansion feedback.

The reactivity feedbacks attempt to adjust the reactor power to match the rate of heat removal from the primary system. Consequently, the absence of heat removal after the first 50 s in the combined loss-of-flow, loss-of-heat-sink case causes the reactor power to decrease much more rapidly. The power, shown in Fig. 6, is nearly a factor of 3 lower at the end of 1000 s than in the first case. As a result, the total energy generation is only about 2/3 of that in the first case. The fuel and coolant temperatures in channel 1 are slightly lower in the second case indicating that the net energy deposition (difference between the total energy generation and the heat removal from the primary system) may also be somewhat lower.

The first two cases show that with the radial expansion feedback as modeled, the reactor can withstand a relatively rapid loss-of-coolant-flow without serious over heating, whether or not heat removal from the primary system occurs. While the calculations cover the first 1000 s after the primary system upset, indications are that this time period could be substantially lengthened. If feedback due to thermally induced

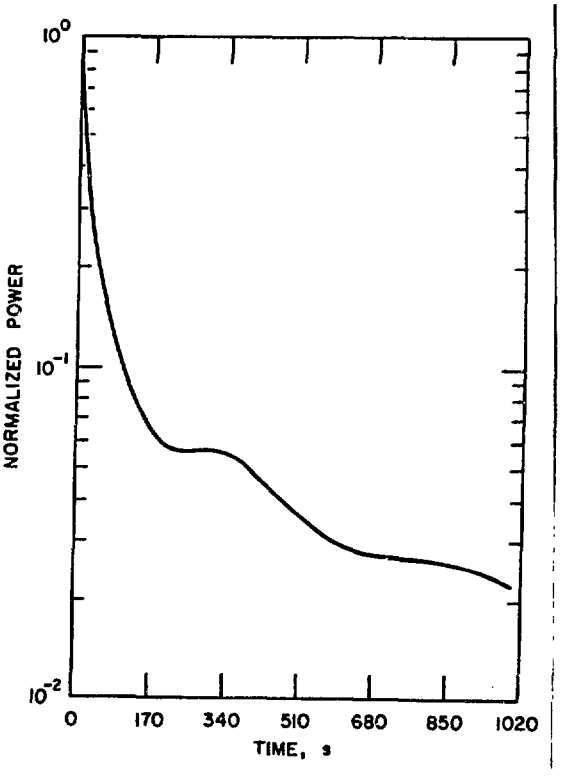

Fig. 6. Reactor power for combined loss-of-flow, loss-of-heat-sink with no control rod reactivity feedback.

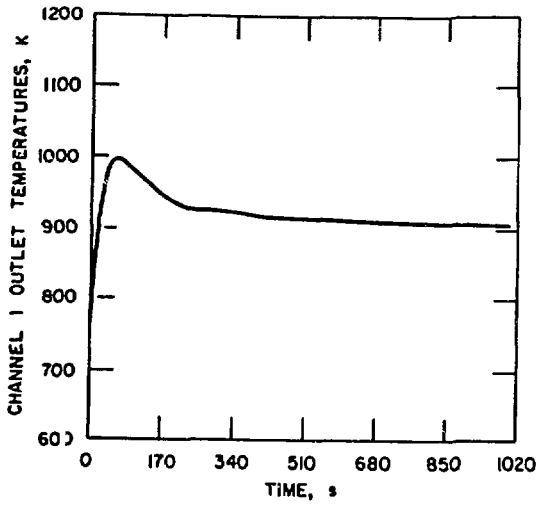

Fig. 7. Coolant outlet temperature for loss-of-flow including control rod reactivity feedback due to drive-line thermal expansion.

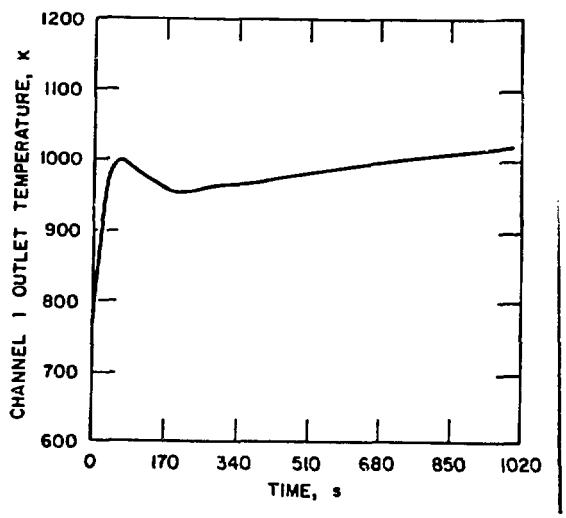

Fig. 8. Coolant outlet temperature for loss-of-flow including control rod reactivity feedback due to drive-line and vessel thermal expansion.

relative motion between the control rods and the core is introduced into the calculation, the reactor response during the first 1000 s changes in detail, but the thermal state of the reactor remains rather similar to that observed in the cases described above. The longer term prospects, however, become sensitive to the design of the control rod support system.

Inclusion of reactivity feedback due to thermal expansion of the control rod drive lines in the calculation for the first case causes a more rapid decrease in the reactor power during the early part of the transient; however, at the end of 1000 s, the power is only 5% of nominal as opposed to the 6% shown in Fig. 2. The fuel, coolant, and structure temperatures are similar to that observed in the first case, but the additional feedback mechanism results in lower values. For example, in Channel 1 at the end of 1000 s, the average fuel temperature near the axial midplane and the coolant and structure temperatures near the subassembly outlet are more than 60 K lower. Furthermore, the rate of temperature increase near the end of the transient is reduced. The coolant and structure temperatures near the outlet are actually decreasing slightly near the end of the transient as shown in Fig. 7.

For the reactor considered here, the ultimate removal of decay heat is by radiative heat transfer from the wall of the reactor vessel. For this heat transfer mechanism to be effective, the vessel wall temperature must increase perhaps a few hundred K. The design of the control rod suspension had not been determined, but to illustrate the effects of a poor design, a fourth case was calculated in which reactivity feedback due to vessel wall expansion was added to the feedbacks considered in the third case. The heated length of the vessel wall was to be about 4 m longer than the heated length of the drive lines. The thermal expansion coefficients for the drive lines and the vessel were assumed to be identical. Because hot sodium reaches the control rod drive lines earlier than it reaches the vessel wall, the control rod feedback remains negative for a little more than 340 s. However, eventually the longer heated length of the vessel dominates and the control rod feedback becomes positive, increasing to more than 40 cents. This positive reactivity contribution must be compensated by radial expansion feedback. As a result, temperatures are higher at the end of the transient than in either the first or the third cases. The coolant and structure temperatures at the outlet of Channel 1 are shown in Fig. 8 and are increasing more rapidly at the end of the transient than in the earlier cases.

Because of the importance of radial expansion reactivity feedback, calculations were done to investivate sensitivity to the parameter X_b in the radial expansion correlation. Control rod feedback was neglected in these calculations. In the first such case, the parameter X_b was reduced to the value $X_b = 1$. The reactor power is plotted in Fig. 9. One sees that the power decreases more slowly during the early part of the transient than Fig. 2, but then catches up and is lower at the end of the transient. Fuel temperatures near the end of the transient are almost 50 K higher than shown in Fig. 4. The coolant and structure temperatures near the outlet of Channel 1, plotted in Fig. 10, have a higher peak value during the first 170 s than seen in Fig. 5, but remain more than 100 K below the sodium boiling temperature. Following the initial increase, these temperatures gradually decrease during the remainder of the transient.

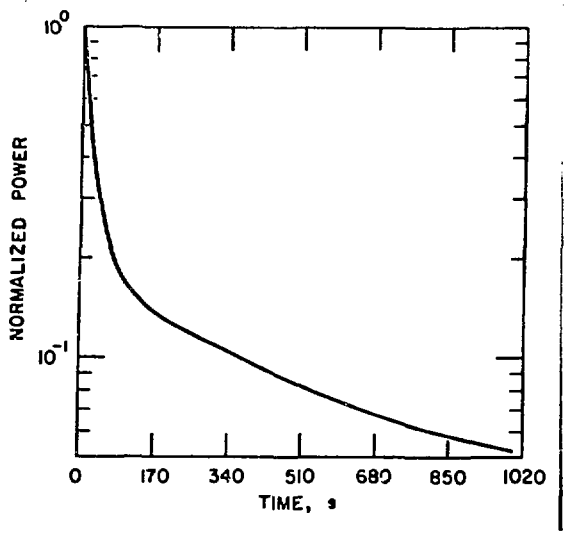

Fig. 9. Reactor power for loss-of-flow with radial expansion parameter X_b = 1.

Recently, this case was rerun with X_b = 0.5 (6), with the result that the nonboiling margin during the first 170 s vanished.

In a second calculation, X_b was set equal to 4. The reactor power for this case exhibited undamped oscillations with a period of almost 200 s. Increasing X_b increases the amplitude while reducing the rate of heat removal lengthens the

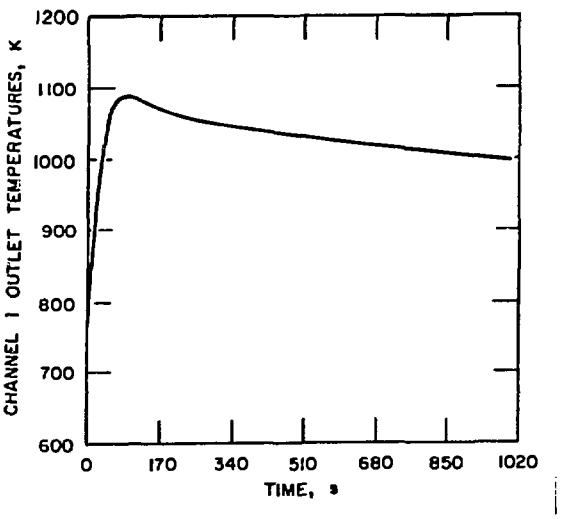

Fig. 10. Coolant outlet temperature for loss-of-flow with radial expansion parameter X_b = 1.

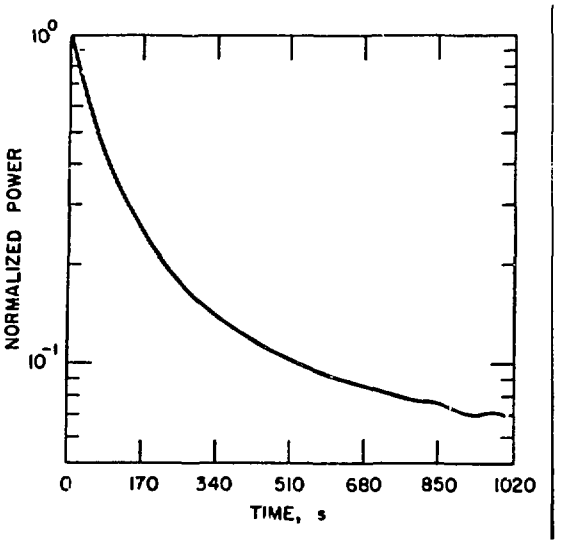

Fig. 11. Reactor power for loss-fo-flow with radial expansion parameter X_b = 6.

period. Coolant boiling initiates in several channels after about 900 s. The cause of the oscillations is, at best, only qualitatively understood. As the flow coasts down, the power-to-flow ratio increases causing a rapid increase in the coolant and structure temperatures near the outlet of the driver fuel subassemblies. The temperature increase leads to large radial expansion reactivity feedback and hence a rapid decrease in the power-to-flow. This allows the fuel temperature to decrease and results in rapidly increasing, positive Doppler and axial expansion feedbacks which coincide with a reduction in the coolant outlet temperature. The combination of rapidly increasing Doppler and axial expansion feedback with the decreasing magnitude of the radial expansion feedback, caused by the decreasing coolant outlet temperature, results in an increase in the net reactivity and brings the reactor to a supercritical state. This causes the power-to-flow to increase again and leads to a repetition of the cycle.

The instability described in the preceding paragraph can be mitigated or eliminated by increasing the halving time of the flow coastdown. The power for a calculation in which X_b = 6 and the flow halving time increased from 3.6 s to 36 s is shown in Fig. 11. The undamped oscillations are no longer observed. Extending the flow coastdown has a second beneficial effect as shown in Fig. 12. The peak in the outlet coolant and structure temperature, observed during the first 170 s in Figs. 5, 7, 8, and 10 is not seen in Fig. 12. This means that early coolant boiling can be avoided with smaller radial expansion reactivity feedback if longer flow coastdowns are used.

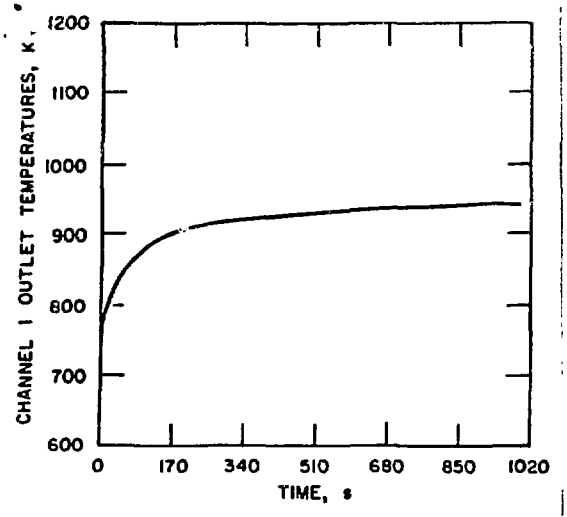

Fig. 12. Coolant outlet temperature for 36 s flow halving time and radial expansion parameter $X_b = 6$.

CONCLUSIONS

The scoping analysis shows that the inherent safety of small, liquid-metal-cooled reactors can be enhanced by accounting for inherent reactivity feedback mechanisms in the design process. For example, the analysis illustrates the importance of understanding radial expansion feedback in setting the flow coastdown time constant. In addition, the results show that the designer should consider thermal expansion of the control rod drive lines relative to the thermal expansion of the vessel wall in designing the control rod suspension system.

Finally, comparison of loss-of-flow cases with combined loss-of-flow, loss-of-heat-sink cases indicates that energy deposition in the reactor during the first 15 to 20 minutes may be less in the combined case than in the loss-of-flow case. This results from the fact that reactivity feedbacks attempt to match the reactor power with the primary system heat removal rate. The calculations show that in either case, with an understanding of inherent reactivity feedback mechanisms, liquid-metal-cooled reactor systems offer the design opportunity of avoiding coolant boiling for extended intervals during unprotected loss-of-flow events.

REFERENCES

1. F. E. Dunn and F. G. Prohammer, "The SASSYS LMFBR Systems Analysis Code," MATHEMATICS AND COMPUTATION IN SIMULATION XXVI, 1984, p. 23.

2. F. E. Dunn and F. G. Prohammer, "SASSYS Analysis of Degraded Shutdown Heat Removal Performance in LMFBRs," ASME paper 82-WA/HT-37, 1982.

3. F. E. Dunn and F. G. Prohammer, "The SASSYS LMFBR Systems Analysis Code," PROCEEDINGS OF THE 10TH IMACS WORLD CONGRESS ON SYSTEM SIMULATION AND SCIENTIFIC COMPUTATION, Vol. 4, Aug. 1982, p. 127.

4. P. R. Huebotter, Private Communication, 1981.

5. J. N. Fox, T. R. Yackle, and P. J. Fulford, "CORTAC - A Core Restraint Transient Analysis Code: User's Mannual," GEAP-14115, Aug. 1976.

6. R. Wigeland, Private Communication, 1985.